

Synthesis, Structure, and Catalytic Hydrogenation Activity of [NO]-Chelate Half-Sandwich Iridium Complexes with Schiff Base Ligands

Wen-Rui Lv, Rong-Jian Li, Zhen-Jiang Liu,* Yan Jin,* and Zi-Jian Yao*

Cite This: *Inorg. Chem.* 2021, 60, 8181–8188

Read Online

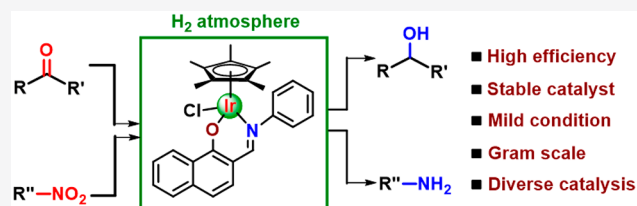
ACCESS |

Metrics & More

Article Recommendations

Supporting Information

ABSTRACT: A series of *N,O*-coordinate iridium(III) complexes with a half-sandwich motif bearing Schiff base ligands for catalytic hydrogenation of nitro and carbonyl substrates have been synthesized. All iridium complexes showed efficient catalytic activity for the hydrogenation of ketones, aldehydes, and nitro-containing compounds using clean H_2 as reducing reagent. The iridium catalyst displayed the highest TON values of 960 and 950 in the hydrogenation of carbonyl and nitro substrates, respectively. Various types of substrates with different substituted groups afforded corresponding products in excellent yields. All *N,O*-coordinate iridium(III) complexes 1–4 were well characterized by IR, NMR, HRMS, and elemental analysis. The molecular structure of complex 1 was further characterized by single-crystal X-ray determination.



INTRODUCTION

Catalytic hydrogenation of nitro-containing substrates and ketones using transition metal catalysts attracted considerable interest in coordination and organometallic chemistry. A number of excellent catalytic hydrogenation systems for the reduction of unsaturated compounds (such as olefins, ketones, and imines) have been exploited and extensively used in pharmaceuticals, organic synthesis, and materials science.¹ Thus, the development of efficient catalysts plays an important role for obtaining high yields and selectivity of the corresponding products. Among different types of reported catalysts, Group 8 and 9 transition metal complexes have been paid much attention because of their activity and stability. Moreover, the good solubility and stability in water of half-sandwich transition metal complexes give the opportunity of their catalytic application in aqueous media.² The physical and chemical properties of these complexes are facily altered through changing the substituted groups in the ligands. Therefore, a number of transition metal complexes containing a half-sandwich motif coordinated with various types of ligands have been prepared and used as hydrogenation precatalysts.^{3–10}

Transition metal complexes based on a half-sandwich structure ($[Cp^*MCl_2]_2$, $Cp^* = Cp^*$, *p*-cymene; $M = Ir, Rh, Ru$) exhibit particular features such as good stability, solubility, and easy functionalization:^{11–15} (i) the half-sandwich transition metal precursors can be prepared smoothly by metal chlorides through facile routes; (ii) Cp^* or cymene ligands shield the hemisphere of the metal center, so the subsequent reactions of these precursors would be easily controlled; (iii) substituted groups bonded to compounds can be readily changed to tune the physical and chemical properties conveniently. The advantages mentioned above made the

half-sandwich motif often used in the synthesis of organometallic complexes.

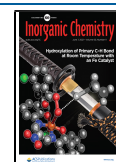
Amines and alcohols are useful intermediates in fine chemicals, the flavor industry, drug synthesis, agricultural sciences, and so on.^{16–19} Reduction of ketones and nitroarenes using stoichiometric $NaBH_4$ or $LiAlH_4$ is an efficient method to prepare amines and alcohols; however, a tremendous amount of waste would be afforded in the meantime. Thus, the transition metal catalyzed hydrogenation process of such substrates using clean H_2 reduction reagent is a more environmentally friendly method in this area. During the past few years, we have concentrated on the synthesis and application of half-sandwich transition metal complexes with different ligands because of their prominent catalytic efficiency. Herein, several *N,O*-chelated mode half-sandwich iridium complexes based on Schiff base ligands were prepared. Experimental results indicated that hydrogenation of both ketones and nitroarenes occurred smoothly under the catalysis of these iridium complexes. All iridium complexes were characterized well, and the influence on the catalytic efficiency of the iridium complexes was investigated.

RESULTS AND DISCUSSION

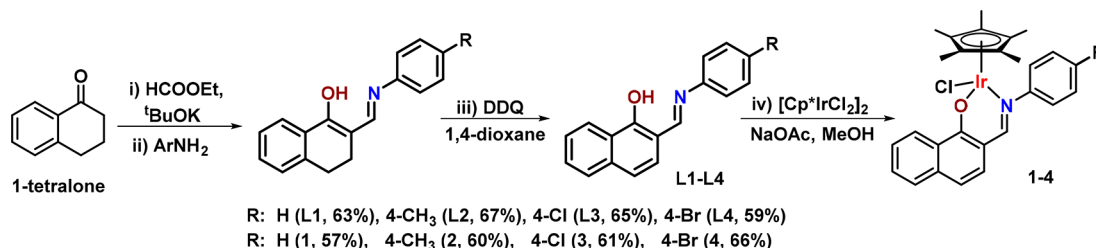
Preparation of Half-Sandwich Iridium(III) Complexes 1–4. Schiff base ligands L1–L4 were obtained through the

Received: March 17, 2021

Published: May 13, 2021



Scheme 1. Synthesis of N,O-Chelate Half-Sandwich Iridium Complexes 1–4



^aReaction conditions: (i) 1-tetralone (1.0 equiv), HCOOEt (1.5 equiv), ^tBuOK (1.5 equiv), 0 °C, 30 min; (ii) aromatic amines (1.1 equiv), HOAc (3 drops), 4 Å MS (0.1 g), MeOH, reflux, 12 h; (iii) DDQ (1.2 equiv), 1,4-dioxane, reflux, 1 h; (iv) [Cp*IrCl₂]₂ (0.5 equiv), NaOAc (2.0 equiv), CH₃OH, reflux, 6 h.

modification processes according to the reported method.²⁰ A β -diketone intermediate was given through the interaction of 1-tetralone and HCOOEt in the presence of the strong base ^tBuOK in anhydrous Et₂O. Then the β -enaminoketonato ligands were obtained through the reactions between corresponding amines and the β -diketones in MeOH catalyzed by HOAc. Ligands L1–L4 were finally obtained by an oxidation reaction of β -enaminoketonato using DDQ as oxidant (Scheme 1). The broad peak at approximately 3415 cm⁻¹ in the IR spectra of the ligands suggests the existence of an -OH group. Four new half-sandwich iridium complexes 1–4 containing N,O-chelate mode ligands were obtained with moderate yields by the interaction of the ligands and iridium precursor [Cp*IrCl₂]₂ promoted by NaOAc in boiling CH₃OH for 6 h (Scheme 1). Pure iridium complexes 1–4 were obtained as dark red powders and exhibited good stability in air for several weeks in the solid state. The iridium complexes showed good solubility in most polar solvents, whereas they are almost insoluble in hexane and Et₂O. Elemental analysis data of the iridium complexes confirmed their expected molecular formula. Good thermal stability of target complexes 1–4 was confirmed by the TGA analysis (see Supporting Information); no decomposition was found at 200 °C.

The singlet at approximately 1.40 ppm was assigned to the protons of the C₅Me₅ group. The characteristic band at 1410–1430 cm⁻¹ in the IR spectra of the iridium complexes 1–4 can be assigned to the signals of the C=N groups of the Schiff base ligand. Compared with the C=N bond vibrations at approximately 1460–1485 cm⁻¹ of the ligands, these signals shifted to lower wavenumbers (1450–1480 cm⁻¹) possibly caused by the coordination between the Ir(III) center and the N donor. The coordination interaction of the iridium complexes could increase the back bonding ability of Ir(III) to the imine bond, and consequently, the electron density on the iridium atom was increased.²¹ All spectroscopy data of the iridium complexes 1–4 indicate their structural similarity.

Molecular Structure of Half-Sandwich Iridium Complex. To elaborate the exact structure of the obtained half-sandwich iridium complex, single-crystal X-ray analysis has been carried out. Qualified single crystals of complex 1 were obtained by the liquid diffusion method between *n*-hexane and a solution of complex 1 in CH₂Cl₂. The molecular structure of complex 1 is shown in Figure 1. Selected geometric data are given in Table 1, and detailed bond lengths and angles are summarized in the caption of Figure 1. The iridium complex exhibited an expected distorted-octahedral environment in which the metal center was chelated by the N, O, and Cl

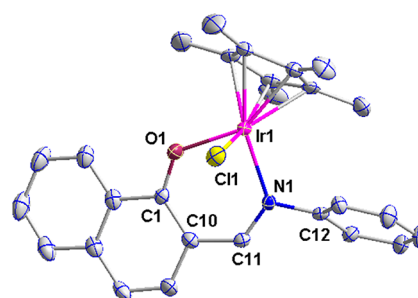


Figure 1. Molecular structure of 1 with thermal ellipsoids drawn at the 30% level. All hydrogen atoms are omitted for clarity. Selected bond lengths (Å) and angles (deg): Ir(1)–N(1), 2.083(4); Ir(1)–O(1), 2.074(4); Ir(1)–Cl(1), 2.4255(12); C(11)–N(1), 1.294(6); C(1)–O(1), 1.299(6); O(1)–Ir(1)–N(1), 87.82(14); O(1)–Ir(1)–Cl(1), 86.89(11); Cl(1)–Ir(1)–N(1), 84.09(11); Ir(1)–O(1)–C(1), 128.6(3); Ir(1)–N(1)–C(11), 126.2(3).

atoms. The excellent stability of the iridium complex may be caused by the formation of the Ir(1)–O(1)–C(1)–C(10)–C(11)–N(1) six-membered ring. The bond lengths of Ir(1)–N(1) and Ir(1)–O(1) of 2.083(4) Å and 2.074(4) Å, respectively, are both located in the normal range of known values.²² The Ir(1)–Cl(1) distance of 2.4255(12) Å is similar to that of the analogous complex.²² The crystal stacking structure of complex 1 does not exhibit any hydrogen bond between molecules.

Catalytic Hydrogenation of Carbonyl Substrates by Iridium Complexes. The catalytic hydrogenation activity of these iridium complexes in the carbonyl compounds' reduction with H₂ as reductive reagent was investigated. Hydrogenation of acetophenone was monitored as the sample to screen the optimal condition. The reaction was carried out at 80 °C with 0.1 mol % catalyst loading in MeOH. The product yields increased from 22% to 96% over 8 h along with the reaction pressure (Table 2, entries 1–5). Six atmospheres is proper for the hydrogenation process, and a further increase of the pressure showed little influence on the hydrogenation process (Table 2, entries 4 and 5). The corresponding alcohol was afforded in good yields at 60 °C for 6 h; however, low conversion was obtained when the catalytic reaction was carried out at room temperature (Table 2, entries 6–10). The reaction gave the best results in MeOH after screening different solvents such as toluene, DMF, THF, and DMSO (Table 2, entries 11–14). The hydrogenation process worked sluggishly in water probably because of the poor solubility of substrate in water (Table 2, entry 15). The product was furnished in 68% yield when 0.05 mol % catalyst loading was

Table 1. Crystallographic Data and Structure Refinement Parameters for **1**^a

	1
Chemical Formula	C ₂₇ H ₂₇ ClIrNO
FW	609.14
T/K	173(2)
λ/Å	0.71073
Crystal system	Monoclinic
Space group	P2(1)/n
a/Å	8.1257(3)
b/Å	12.3595(6)
c/Å	23.0291(11)
α/deg	90
β/deg	92.595(2)
γ/deg	90
V/Å ³	2310.43(18)
Z	4
ρ/Mg m ⁻³	1.751
μ/mm ⁻¹	5.914
F(000)	1192
θ range/deg	2.419–26.817
Reflections collected	66015
Data/restraints/param	4930/0/285
Goodness-of-fit on F ²	1.069
Final R indices [I > 2σ(I)] ^a	R1 = 0.0340 wR2 = 0.0963
Largest diff.peak/hole (e Å ⁻³)	1.314/−1.807

^aR₁ = $\sum ||F_o| - |F_c|| / \sum |F_o|$ (based on reflections with $F_o^2 > 2\sigma F^2$). wR_2 = $[\sum [w(F_o^2 - F_c^2)^2] / \sum [w(F_o^2)^2]]^{1/2}$; $w = 1/[\sigma^2(F_o^2) + (0.095P)^2]$; $P = [\max(F_o^2, 0) + 2F_c^2]/3$ (also with $F_o^2 > 2\sigma F^2$).

used in the reaction (Table 2, entry 16). All the iridium complexes were used in the hydrogenation reaction under the optimal conditions and little differences of catalytic activity were observed (Table 2, entries 17–19). Little product was found when the reaction was carried out under the catalysis of [Cp*IrCl₂]₂ or in the absence of the catalyst (Table 2, entries 20 and 21).

We subsequently investigated the generality of the reaction after the optimal conditions were obtained. A survey of various types of ketones and aldehydes was investigated in the hydrogenation process. Generally, all aromatic substrates reacted well in such conditions, and the corresponding aromatic alcohols were furnished in excellent yields (Table 3, **5a–5p**). A stereoselectivity study was carried out by employing *ortho*-, *meta*-, and *para*-methylacetophenone in the reaction aiming to elaborate the influence of the substituent position on the catalysis; to our delight, all reactions occurred smoothly under such conditions (Table 3, **5e–g**). High yields of the alcohols were also observed when bulky substituent bonded substrates were used in the reaction (Table 3, **5l** and **5m**). Additionally, heteroaromatic aldehydes with pyridine and furan moieties were reduced efficiently under catalysis of iridium complex **1** (Table 3, **5q** and **5r**). In comparison with the aromatic substrates, aliphatic aldehydes and ketones were less reactive and their hydrogenation process required harsh conditions such as higher temperature and longer reaction time to get good results (Table 3, **5s–5u**). The catalytic system showed high efficiency on the hydrogenation of the carbonyl group, whereas the ester group was intact in the reaction (Table 3, **5u**).

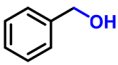
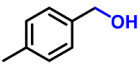
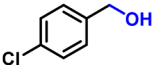
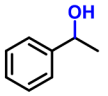
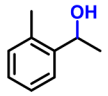
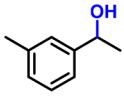
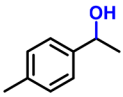
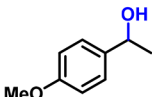
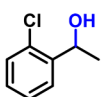
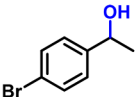
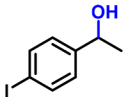
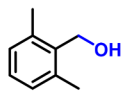
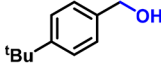
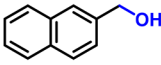
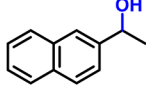
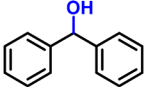
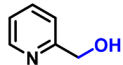
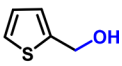
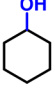
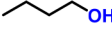
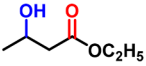
The interaction between the iridium catalyst and H₂ was monitored to explore the plausible mechanism of this reaction.

Table 2. Catalytic Hydrogenation of Acetophenone under Catalysis of Iridium Complexes **1–4**^a

entry	Cat.(mol %)	T/°C	H ₂ /atm	Time/h	Solvent	Yield/% ^b	TON	TOF
1	1 (0.1)	80	1	8	MeOH	22	220	27.5
2	1 (0.1)	80	2	8	MeOH	39	390	48.8
3	1 (0.1)	80	4	8	MeOH	72	720	90.0
4	1 (0.1)	80	6	8	MeOH	96	960	120.0
5	1 (0.1)	80	8	8	MeOH	96	960	120.0
6	1 (0.1)	60	6	8	MeOH	96	960	120.0
7	1 (0.1)	40	6	8	MeOH	61	610	76.3
8	1 (0.1)	rt	6	8	MeOH	15	150	18.8
9	1 (0.1)	60	6	6	MeOH	95	950	158.3
10	1 (0.1)	60	6	3	MeOH	69	690	230.0
11	1 (0.1)	60	6	6	toluene	53	530	88.3
12	1 (0.1)	60	6	6	DMF	77	770	128.3
13	1 (0.1)	60	6	6	THF	38	380	63.3
14	1 (0.1)	60	6	6	DMSO	71	710	118.3
15	1 (0.1)	60	6	6	H ₂ O	42	420	70.0
16	1 (0.05)	60	6	6	MeOH	68	1360	226.7
17	2 (0.1)	60	6	6	MeOH	95	950	158.3
18	3 (0.1)	60	6	6	MeOH	93	930	155.0
19	4 (0.1)	60	6	6	MeOH	93	930	155.0
20		60	6	6	MeOH			
21	[Cp*IrCl ₂] ₂	60	6	6	MeOH	trace		

^aReaction conditions: an autoclave was charged with the catalyst and solvent (2.0 mL), followed by acetophenone (1.0 mmol) under Ar. The autoclave was then charged with H₂ and heated in an oil bath. ^bYield was determined by GC analysis.

Table 3. Catalytic Hydrogenation of Carbonyl Substrates^a

$\text{R}_1-\text{C}(=\text{O})-\text{R}_2 \xrightarrow[60\text{ }^\circ\text{C, 6 h, MeOH (2 mL)}]{1\text{ (0.1 mol\%)} , \text{H}_2\text{ (6 atm)}} \text{R}_1-\text{CH}(\text{OH})-\text{R}_2$					
					
5a 97% (93% ^b)	5b 95% (91%)	5c 96% (92%)	5d 95% (90%)	5e 91% (87%)	5f 91% (86%)
					
5g 92% (87%)	5h 93% (87%)	5i 96% (91%)	5j 95% (91%)	5k 96% (90%)	5l 91% (85%)
					
5m 92% (88%)	5n 97% (93%)	5o 93% (89%)	5p 95% (90%)	5q 92% (87%)	5r 93% (87% ^b)
	5s 82% (77% ^b)		5t 80% (74% ^b)		5u 83% (79% ^b)

^aReaction conditions: an autoclave was charged with complex **1** (0.1 mol %) and MeOH (2.0 mL), followed by ketone (1 mmol). The autoclave was then charged with H₂ (6 atm). Six hours at 60 °C in an oil bath. Yield was determined by GC analysis. Isolated yields (%) are provided in parentheses. ^bReaction conditions: 80 °C, 12 h.

The NMR tube containing a dry C₆D₆ solution of complex **1** was charged with H₂ (6 atm). Then the mixture was reacted at 60 °C and a singlet was observed at very high field, which suggests the generation of metal hydride intermediates.²³ We speculate that the loss of chloride ligand occurred under high H₂ pressure atmosphere at elevated temperature. A similar phenomenon was observed in the ruthenium complex catalyzed hydrogenation process.²⁴ It was concluded from the condition screening stage that the catalytic hydrogenation process benefits from higher reaction pressure. Figure 2

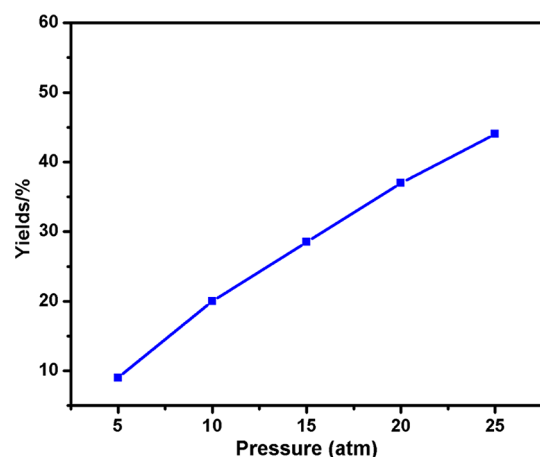


Figure 2. Influence of H₂ pressure on the catalytic hydrogenation process. Reaction conditions: 1.0 mmol of acetophenone, 0.1 mol % of iridium catalyst **1**, H₂, 60 °C for 1 h. The conversion was determined by GC.

indicates a linear correlation between reaction pressure and conversions, suggesting H₂ heterolytic cleavage and the formation of the metal hydrides are possibly involved in the rate-determining step of this catalytic reaction.

The plausible catalytic mechanism was proposed based on the results mentioned above. The heterolytic cleavage of H₂ induced by iridium catalyst occurred to give the iridium hydride intermediate under high pressure and elevated reaction temperature. The catalytic hydrogenation cycle is composed of the following steps: (i) reversible coordination of H₂ to the iridium complex; (ii) turnover-limiting heterolytic cleavage of H₂ to give the Ir–H intermediate and the addition of the proton to the carbonyl group; (iii) transfer of the hydride to the carbon atom of the oxonium cation (Figure 3).^{25,26}

Catalytic Hydrogenation of Nitro-Containing Compounds. Reduction of nitroarenes represents a direct and efficient route to synthesize amines in various types of synthetic methodologies.²⁷ The catalytic efficiency of complex **1** in nitroarenes' hydrogenation was also investigated. Fortunately, hydrogenation of nitroarenes occurred smoothly in the presence of iridium catalyst **1** under the optimal conditions mentioned above. The electronic effects of the substituents do not exhibit an obvious influence on the catalytic efficiency; corresponding amines were all given in moderate to good yields (Table 4, 6a–6l). However, reduction of substrates with steric hindrance groups such as 2,6-diisopropylbenzene was not good and 2,6-diisopropylaniline was furnished with lower yield (Table 4, 6m). Unsaturated groups such as –CN, –COOR, and COOH were intact under such conditions, which indicated the high selectivity of this reaction (Table 4, 6e, 6k, and 6l). A lower yield of 4-aminobenzoic acid was probably caused by the instability of

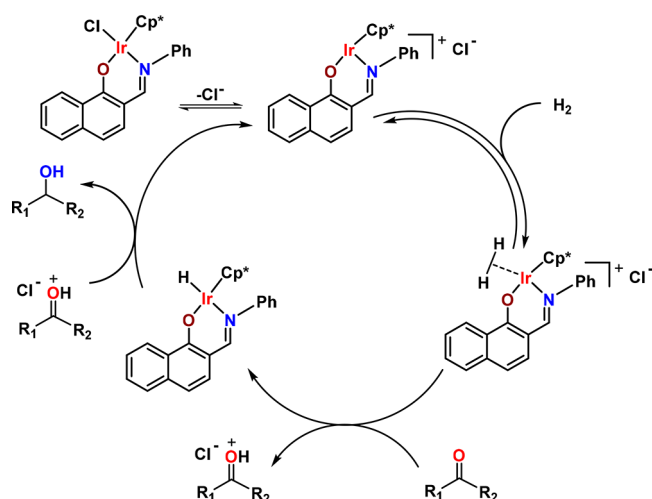


Figure 3. Possible mechanism of the catalytic hydrogenation process.

the iridium catalyst in acidic conditions (Table 4, **6l**). Aliphatic substrate displayed slightly low reactivity in the catalytic hydrogenation process (Table 4, **6n** and **6o**). Moreover, reactions of polynitro compounds gave positive results (Table 4, **6p–6r**).

CONCLUSIONS

In summary, a series of N,O-chelate half-sandwich iridium complexes based on Schiff-containing Schiff base ligands have been prepared and characterized. Such air-stable complexes exhibit good and diverse catalytic hydrogenation activity for carbonyl and nitro-containing compounds by using clean H₂ as the reduce reagent. Various types of substrates with different substituted groups afforded corresponding products in excellent yields under optimal conditions. Experimental results indicate that metal hydride formation is the rate-determining step in the catalytic hydrogenation process. Further study of

the effect of the catalytic system on other hydrogenation processes is currently underway.

EXPERIMENTAL SECTION

General Data. All manipulations were performed under an atmosphere of nitrogen using standard Schlenk techniques. Chemicals were used as commercial products without further purification. ¹H NMR (500 MHz) spectra were measured with a Bruker DMX-500 spectrometer. Elemental analysis was performed on an Elementar vario EL III analyzer. IR (KBr) spectra were measured with the Nicolet FT-IR spectrophotometer. Electrospray ionization mass spectrometry was carried out on a Waters API Quattro Micro triple quadrupole mass spectrometer in the positive ion mode.

Synthesis of Schiff Base Ligands L1–L4. ^tBuOK (6.5 g, 1.5 equiv), 1-tetralone (8.8 g, 40.0 mmol), and ethyl formate (5.8 g, 2.0 equiv) were stirred at 0 °C in ethyl ether (100 mL) for 30 min. Then the reaction mixture was warmed to room temperature and stirred for another 10 h. The precipitate was filtered and washed by Et₂O (20 mL); then the crude product was dried under vacuum. HCOOH was added to the product until pH < 7. Then aromatic amine (1.0 equiv) was added to the acidic solution, and the mixture was stirred for 24 h to generate the corresponding β-enaminoketonato as a yellow solid. The obtained β-enaminoketonato was mixed with DDQ (1.1 equiv), and the mixture was refluxing in dioxane for 1 h. The reaction was then monitored by TLC. Column chromatography of the crude products (PE: EA = 6:1) gave **L1–L4** in good yields.

L1. White solid, 63% isolated yield. ¹H NMR (500 MHz, CDCl₃): δ 14.89 (s, 1H), 8.47 (d, *J* = 8.1 Hz, 1H), 8.40 (d, *J* = 5.4 Hz, 1H), 7.65 (d, *J* = 7.9 Hz, 1H), 7.59 (t, *J* = 7.3 Hz, 1H), 7.50–7.42 (m, 3H), 7.34 (d, *J* = 7.8 Hz, 2H), 7.28 (s, 1H), 7.14 (d, *J* = 8.7 Hz, 1H), 7.01 (d, *J* = 8.7 Hz, 1H) ppm. IR (KBr, disk): ν 3423, 1668, 1545, 1530, 1472, 1356, 752 cm^{−1}. Elemental analysis calcd (%) for C₁₇H₁₃NO: C 82.57, H 5.30, N 5.66, found: C 82.65, H 5.38, N 5.60.

L2. White solid, 67% isolated yield. ¹H NMR (500 MHz, CDCl₃): δ 8.49–8.35 (m, 2H), 7.68 (d, *J* = 8.0 Hz, 1H), 7.59 (t, *J* = 7.0 Hz, 1H), 7.49 (t, *J* = 7.2 Hz, 1H), 7.39 (d, *J* = 8.7 Hz, 2H), 7.29–7.26 (m, 1H), 7.25 (s, 1H), 7.18 (d, *J* = 8.7 Hz, 1H), 7.10 (d, *J* = 8.7 Hz, 1H) ppm. IR (KBr, disk): ν 3450, 1625, 1575, 1533, 1485, 1302, 755 cm^{−1}. Elemental analysis calcd (%) for C₁₈H₁₅NO: C 82.73, H 5.79, N 5.36, found: C 82.68, H 5.72, N 5.41.

Table 4. Catalytic Hydrogenation of Nitro Substrates^a

$\text{R}-\text{C}_6\text{H}_4-\text{NO}_2 \xrightarrow[60^\circ\text{C, 6 h, MeOH (2 mL)}]{1 (0.1 \text{ mol\%}), \text{H}_2 (6 \text{ atm})} \text{R}-\text{C}_6\text{H}_4-\text{NH}_2$					
6a 95% (91%)	6b 92% (87%)	6c 94% (90%)	6d 95% (90%)	6e 89% (84%)	6f 87% (81%)
6g 95% (90%)	6h 96% (91%)	6i 93% (88%)	6j 93% (88%)	6k 92% (88%)	6l 82% (77%)
6m 83% (78%)	6n 79% (75%)	6o 78% (75%)	6p 88% (82%)	6q 85% (81%)	6r 88% (83%)

^aReaction conditions: an autoclave was charged with complex **1** (0.1 mol %) and MeOH (2.0 mL), followed by nitroarenes (1 mmol). The autoclave was then charged with H₂ (6 atm). Six hours at 60 °C in an oil bath. Yield was determined by GC analysis. Isolated yields (%) are provided in parentheses.

L3. White solid, 65% isolated yield. ^1H NMR (500 MHz, CDCl_3): δ 8.45 (d, J = 8.1 Hz, 2H), 7.69 (d, J = 7.9 Hz, 1H), 7.62–7.54 (m, 3H), 7.50 (t, J = 7.5 Hz, 1H), 7.21 (t, J = 8.7 Hz, 3H), 7.11 (d, J = 8.7 Hz, 1H) ppm. IR (KBr, disk): ν 3425, 1606, 1561, 1513, 1460, 1363, 1271, 759 cm^{-1} . Elemental analysis calcd (%) for $\text{C}_{17}\text{H}_{12}\text{ClNO}$: C 72.47, H 4.29, N 4.97, found: C 72.55, H 4.32, N 5.03.

L4. White solid, 59% isolated yield. ^1H NMR (500 MHz, CDCl_3): δ 8.47 (d, J = 8.1 Hz, 1H), 8.39 (s, 1H), 7.65 (d, J = 8.0 Hz, 1H), 7.58 (t, J = 7.5 Hz, 1H), 7.47 (t, J = 7.5 Hz, 1H), 7.24 (s, 4H), 7.14 (d, J = 8.7 Hz, 1H), 7.01 (d, J = 8.7 Hz, 1H), 2.38 (s, 3H) ppm. IR (KBr, disk): ν 3439, 1630, 1556, 1470, 1308, 1263, 1125, 765 cm^{-1} . Elemental analysis calcd (%) for $\text{C}_{17}\text{H}_{12}\text{BrNO}$: C 62.60, H 3.71, N 4.29, found: C 62.65, H 3.73, N 4.25.

Synthesis of Half-Sandwich Iridium Complexes 1–4. A mixture of $[\text{Cp}^*\text{IrCl}_2]_2$ (0.1 mmol), NaOAc (0.4 mmol), and Schiff base ligands **L1–L4** (0.2 mmol) was stirred at 65 $^\circ\text{C}$ in 10 mL of methanol for 6 h. The mixture was filtered and evaporated to give the crude products which were further purified by silica gel column chromatography (PE:EA = 4:1) to afford the half-sandwich iridium complexes.

1. Red solid, 57% isolated yield. ^1H NMR (500 MHz, CDCl_3): δ 8.64 (d, J = 8.2 Hz, 1H), 8.05 (s, 1H), 7.68 (d, J = 7.7 Hz, 2H), 7.54 (dd, J = 13.4, 6.4 Hz, 2H), 7.42–7.33 (m, 4H), 7.04 (d, J = 8.6 Hz, 1H), 6.82 (d, J = 8.7 Hz, 1H), 1.38 (s, 15H) ppm. ^{13}C NMR (125 MHz, CDCl_3): δ 162.5, 159.6, 155.9, 137.8, 130.3, 129.7, 128.8, 128.4, 127.3, 126.9, 125.9, 125.2, 124.7, 114.5, 113.1, 86.0, 8.6 ppm. IR (KBr, disk): ν 1755, 1636, 1574, 1506, 1422, 1359, 769 cm^{-1} . Elemental analysis calcd (%) for $\text{C}_{27}\text{H}_{27}\text{NOClIr}$: C 52.23, H 4.47, N 2.30, found: C 52.28, H 4.49, N 2.23. HRMS calcd for $[\text{M}-\text{Cl}]^+$: m/z 574.1722; found: 574.1729.

2. Red solid, 60% isolated yield. ^1H NMR (500 MHz, CDCl_3): δ 8.63 (d, J = 8.3 Hz, 1H), 7.99 (s, 1H), 7.66 (d, J = 8.6 Hz, 2H), 7.55 (d, J = 6.9 Hz, 2H), 7.37 (t, J = 7.3 Hz, 3H), 7.02 (d, J = 8.7 Hz, 1H), 6.82 (d, J = 8.7 Hz, 1H), 1.40 (s, 15H) ppm. ^{13}C NMR (125 MHz, CDCl_3): δ 162.7, 159.6, 154.4, 137.9, 132.4, 130.2, 129.6, 128.9, 128.4, 127.3, 126.6, 125.9, 124.8, 114.8, 113.1, 86.1, 8.7 ppm. IR (KBr, disk): ν 1715, 1652, 1563, 1485, 1410, 1358, 856, 763 cm^{-1} . Elemental analysis calcd (%) for $\text{C}_{28}\text{H}_{29}\text{NOClIr}$: C 53.96, H 4.69, N 2.25, found: C 54.03, H 4.65, N 2.29. HRMS calcd for $[\text{M}-\text{Cl}]^+$: m/z 588.1878; found: 588.1870.

3. Red solids, 61% isolated yield. ^1H NMR (500 MHz, CDCl_3): δ 8.62 (d, J = 8.2 Hz, 1H), 7.99 (s, 1H), 7.59 (t, J = 7.0 Hz, 3H), 7.53 (dd, J = 10.8, 5.7 Hz, 3H), 7.39 (d, J = 6.3 Hz, 1H), 7.02 (d, J = 8.7 Hz, 1H), 6.82 (d, J = 8.7 Hz, 1H), 1.40 (s, 15H) ppm. ^{13}C NMR (125 MHz, CDCl_3): δ 162.8, 159.5, 154.8, 137.9, 131.4, 130.2, 129.6, 128.9, 127.3, 126.9, 125.9, 124.8, 120.3, 114.8, 113.1, 86.0, 8.7 ppm. IR (KBr, disk): ν 1745, 1634, 1555, 1502, 1419, 1354, 863, 755 cm^{-1} . Elemental analysis calcd (%) for $\text{C}_{27}\text{H}_{26}\text{Cl}_2\text{NOIr}$: C 50.39, H 4.07, N 2.18, found: C 50.33, H 4.11, N 2.25. HRMS calcd for $[\text{M}-\text{Cl}]^+$: m/z 608.1332; found: 608.1341.

4. Red solids, 66% isolated yield. ^1H NMR (500 MHz, CDCl_3): δ 8.64 (d, J = 8.2 Hz, 1H), 8.02 (s, 1H), 7.57–7.53 (m, 4H), 7.37 (t, J = 7.1 Hz, 1H), 7.17 (d, J = 8.0 Hz, 2H), 7.04 (d, J = 8.6 Hz, 1H), 6.82 (d, J = 8.6 Hz, 1H), 2.40 (s, 3H), 1.38 (s, 15H) ppm. ^{13}C NMR (125 MHz, CDCl_3): δ 162.3, 159.4, 153.7, 137.8, 136.6, 130.4, 129.6, 128.9, 128.7, 127.3, 125.9, 124.9, 124.6, 114.4, 113.1, 86.0, 21.0, 8.6 ppm. IR (KBr, disk): ν 1723, 1600, 1574, 1504, 1430, 1356, 871, 765 cm^{-1} . Elemental analysis calcd (%) for $\text{C}_{27}\text{H}_{26}\text{BrNOClIr}$: C 47.13, H 3.81, N 2.04, found: C 47.18, H 3.87, N 1.96. HRMS calcd for $[\text{M}-\text{Cl}]^+$: m/z 652.0827; found: 652.0833.

General Procedure for Catalytic Hydrogenation of Carbonyl Substrates. In a typical run, the substrate (1.0 mmol), iridium complex **1** (0.1 mol %), and MeOH (2 mL) were charged in a 5 mL vial with a magnetic bar. The vial was then transferred to an autoclave. The autoclave was purged with H_2 (6 atm) via three cycles. The autoclave was heated to 60 $^\circ\text{C}$. After stirring for 6 h, the autoclave was cooled and the pressure was slowly released. The resultant mixture was extracted with diethyl ether (2 \times 5 mL) and dried over anhydrous Na_2SO_4 . Solvent was evaporated under vacuum. The residue was dissolved in hexane and analyzed by GC-MS.

General Procedure for Catalytic Hydrogenation of Nitroarenes. In a typical run, the substrate (1.0 mmol), iridium complex **1** (0.1 mol %), and MeOH (2 mL) were charged in a 5 mL vial with a magnetic bar. The vial was then transferred to an autoclave. The autoclave was purged with H_2 (6 atm) via three cycles. The autoclave was heated to 60 $^\circ\text{C}$. After stirring for 6 h, the autoclave was cooled and the pressure was slowly released. The resultant mixture was extracted with diethyl ether (2 \times 5 mL) and dried over anhydrous Na_2SO_4 . Solvent was evaporated under vacuum. The residue was dissolved in hexane and analyzed by GC-MS.

X-ray Crystallography. Diffraction data of **1** were collected on a Bruker Smart APEX CCD diffractometer with graphite-monochromated Mo K α radiation (λ = 0.71073 Å). All the data were collected at room temperature, and the structures were solved by direct methods and subsequently refined on F^2 by using full-matrix least-squares techniques (SHELXL).²⁸ SADABS²⁹ absorption corrections were applied to the data, all non-hydrogen atoms were refined anisotropically, and hydrogen atoms were located at calculated positions. All calculations were performed using the Bruker program Smart.

■ ASSOCIATED CONTENT

Supporting Information

The Supporting Information is available free of charge at <https://pubs.acs.org/doi/10.1021/acs.inorgchem.1c00820>.

^1H NMR spectra of **L1–L4**; ^1H NMR and ^{13}C NMR spectra of complexes **1–4**; TGA curves of complexes **1–4** (PDF)

Accession Codes

CCDC 2058746 contains the supplementary crystallographic data for this paper. These data can be obtained free of charge via www.ccdc.cam.ac.uk/data_request/cif, or by emailing data_request@ccdc.cam.ac.uk, or by contacting The Cambridge Crystallographic Data Centre, 12 Union Road, Cambridge CB2 1EZ, UK; fax: +44 1223 336033.

■ AUTHOR INFORMATION

Corresponding Authors

Zi-Jian Yao – School of Chemical and Environmental Engineering, Shanghai Institute of Technology, Shanghai 201418, China; Key Lab of Synthetic Chemistry of Natural Substances, Shanghai Institute of Organic Chemistry, Chinese Academy of Sciences, Shanghai 200032, China; orcid.org/0000-0003-1833-1142; Phone: +86-21-60877231; Email: zjyao@sit.edu.cn; Fax: +86-21-60877335

Zhen-Jiang Liu – School of Chemical and Environmental Engineering, Shanghai Institute of Technology, Shanghai 201418, China; orcid.org/0000-0001-6850-9485; Email: zjliu@sit.edu.cn

Yan Jin – College of Sciences, Shanghai Institute of Technology, Shanghai 201418, China; Key Laboratory of Wireless Sensor Network & Communication, Shanghai Institute of Microsystem and Information Technology, Chinese Academy of Sciences, Shanghai 200050, China; Email: jinyan@sit.edu.cn

Authors

Wen-Rui Lv – School of Chemical and Environmental Engineering, Shanghai Institute of Technology, Shanghai 201418, China; Key Laboratory of Wireless Sensor Network & Communication, Shanghai Institute of Microsystem and Information Technology, Chinese Academy of Sciences, Shanghai 200050, China

Rong-Jian Li – School of Chemical and Environmental Engineering, Shanghai Institute of Technology, Shanghai 201418, China

Complete contact information is available at:
<https://pubs.acs.org/10.1021/acs.inorgchem.1c00820>

Notes

The authors declare no competing financial interest.

ACKNOWLEDGMENTS

This work was supported by the National Natural Science Foundation of China (No. 21601125), the Chenguang Scholar of Shanghai Municipal Education Commission (No. 16CG64), the Shanghai Gaofeng & Gaoyuan Project for University Academic Program Development, and the research funding of Shanghai Institute of Technology (ZQ2020-10).

REFERENCES

- (1) *The Handbook of Homogeneous Hydrogenation*; de Vries, J. G., Elsevier, C. J., Eds.; Wiley-VCH: Weinheim, 2007.
- (2) (a) Schmitt, F.; Freudenreich, J.; Barry, N. P. E.; Juillerat-Jeanneret, L.; Süss-Fink, G.; Therrien, B. Organometallic Cages as Vehicles for Intracellular Release of Photosensitizers. *J. Am. Chem. Soc.* **2012**, *134*, 754–757. (b) Palmucci, J.; Marchetti, F.; Pettinari, R.; Pettinari, C.; Scopelliti, R.; Riedel, T.; Therrien, B.; Galindo, A.; Dyson, P. J. Synthesis, Structure, and Anticancer Activity of Arene–Ruthenium(II) Complexes with Acylpyrazolones Bearing Aliphatic Groups in the Acyl Moiety. *Inorg. Chem.* **2016**, *55*, 11770–11781. (c) Gatti, A.; Habtemariam, A.; Romero-Canelón, I.; Song, J.-L.; Heer, B.; Clarkson, G. J.; Rogolino, D.; Sadler, P. J.; Carcelli, M. Half-Sandwich Arene Ruthenium(II) and Osmium(II) Thiosemicarbazone Complexes: Solution Behavior and Antiproliferative Activity. *Organometallics* **2018**, *37*, 891–899. (f) Robertson, A.; Matsumoto, T.; Ogo, S. The development of aqueous transfer hydrogenation catalysts. *Dalton Trans.* **2011**, *40*, 10304–10310. (g) Crochet, P.; Cadierno, V. Arene-ruthenium(II) complexes with hydrophilic P-donor ligands: versatile catalysts in aqueous media. *Dalton Trans.* **2014**, *43*, 12447–12462. (h) Süss-Fink, G. Water-soluble arene ruthenium complexes: From serendipity to catalysis and drug design. *J. Organomet. Chem.* **2014**, *751*, 2–19. (i) Foubelo, F.; Nájera, C.; Yus, M. Catalytic asymmetric transfer hydrogenation of ketones: recent advances. *Tetrahedron: Asymmetry* **2015**, *26*, 769–790. (j) Mannancheril, V.; Therrien, B. Strategies toward the Enhanced Permeability and Retention Effect by Increasing the Molecular Weight of Arene Ruthenium Metallaassemblies. *Inorg. Chem.* **2018**, *57*, 3626–3633. (k) Garci, A.; Mbakidi, J.-P.; Chaleix, V.; Sol, V.; Orhan, E.; Therrien, B. Tunable Arene Ruthenium Metallaassemblies to Transport, Shield, and Release Porphyrin in Cancer Cells. *Organometallics* **2015**, *34*, 4138–4146. (l) Pitto-Barry, A.; Barry, N. P. E.; Russo, V.; Heinrich, B.; Donnio, B.; Therrien, B.; Deschenaux, R. Designing Supramolecular Liquid-Crystalline Hybrids from Pyrenyl-Containing Dendrimers and Arene Ruthenium Metallaassemblies. *J. Am. Chem. Soc.* **2014**, *136*, 17616–17625. (m) Wang, C.; Zhao, W.; Cao, B.; Wang, Z.; Zhou, Q.; Lu, S.; Lu, L.; Zhan, M.; Hu, X. Biofilm-responsive Polymeric Nanoparticles with Self-adaptive Deep Penetration for In Vivo Photothermal Treatment of Implant Infection. *Chem. Mater.* **2020**, *32*, 7725–7738. (n) Chu, C.; Lyu, X.; Wang, Z.; Jin, H.; Lu, S.; Xing, D.; Hu, X. Cocktail Polyprodrug Nanoparticles to Concurrently Pump out Nitric Oxide and Peroxynitrite against Cisplatin-Resistant Cancers. *Chem. Eng. J.* **2020**, *402*, 126125.
- (3) Talwar, D.; Li, H. Y.; Durham, E.; Xiao, J. A Simple Iridacycle Catalyst for Efficient Transfer Hydrogenation of N-Heterocycles in Water. *Chem. - Eur. J.* **2015**, *21*, 5370–5379.
- (4) Zhou, X.; Wu, X.-F.; Yang, B.-L.; Xiao, J. Varying the Ratio of Formic Acid to Triethylamine Impacts on Asymmetric Transfer Hydrogenation of Ketones. *J. Mol. Catal. A: Chem.* **2012**, *357*, 133–140.
- (5) Chen, H.-Y. T.; Wang, C.; Wu, X.; Jiang, X.; Catlow, C. R. A.; Xiao, J. Iridacycle-Catalysed Imine Reduction: An Experimental and Computational Study of the Mechanism. *Chem. - Eur. J.* **2015**, *21*, 16564–16577.
- (6) Liu, J.; Wu, X.; Iggo, J. A.; Xiao, J. Half-sandwich Iridium Complexes-Synthesis and Applications in Catalysis. *Coord. Chem. Rev.* **2008**, *252*, 782–809.
- (7) Wang, C.; Xiao, J. Iridacycles for Hydrogenation and Dehydrogenation reactions. *Chem. Commun.* **2017**, *53*, 3399–3411.
- (8) Wang, C.; Pettman, A.; Basca, J.; Xiao, J. A Versatile Catalyst for Reductive Amination by Transfer Hydrogenation. *Angew. Chem., Int. Ed.* **2010**, *49*, 7548–7552.
- (9) Nandhini, R.; Krishnamoorthy, B. S.; Venkatachalam, G. Binuclear half-sandwich ruthenium(II) Schiff base complexes: Synthesis, characterization, DFT study and catalytic activity for the reduction of nitroarenes. *J. Organomet. Chem.* **2019**, *903*, 120984.
- (10) Yao, Z.-J.; Zhu, J.-W.; Lin, N.; Qiao, X.-C.; Deng, W. Catalytic hydrogenation of carbonyl and nitro compounds using an [N,O]-chelate half-sandwich ruthenium catalyst. *Dalton Trans.* **2019**, *48*, 7158–7166.
- (11) (a) Han, Y.-F.; Jin, G.-X. Half-Sandwich Iridium- and Rhodium-based Organometallic Architectures: Rational Design, Synthesis, Characterization, and Applications. *Acc. Chem. Res.* **2014**, *47*, 3571–3579. (b) Han, Y.-F.; Jin, G.-X. Cyclometalated [Cp**M*-(C[∧]X)] (*M* = Ir, Rh; X = N, C, O, P) complexes. *Chem. Soc. Rev.* **2014**, *43*, 2799–2823.
- (12) (a) Zhang, R.; Zhu, L.; Liu, G.; Dai, H.; Lu, Z.; Zhao, J.; Yan, H. Cobalt-Promoted B-H and C-H Activation: Facile B-C Coupling of Carboranedithiolate and Cyclopentadienyl. *J. Am. Chem. Soc.* **2012**, *134*, 10341–10344. (b) Wang, Z.; Ye, H.; Li, Y.; Li, Y.; Yan, H. Unprecedented Boron-Functionalized Carborane Derivatives by Facile and Selective Cobalt-Induced B-H Activation. *J. Am. Chem. Soc.* **2013**, *135*, 11289–11298.
- (13) Kumar, P.; Gupta, R. K.; Pandey, D. S. Half-sandwich arene ruthenium complexes: synthetic strategies and relevance in catalysis. *Chem. Soc. Rev.* **2014**, *43*, 707–733.
- (14) Gichumbi, J. M.; Friedrich, H. B.; Omondi, B. Synthesis and characterization of piano-stool ruthenium complexes with *N,N'*-pyridine imine bidentate ligands and their application in styrene oxidation. *J. Organomet. Chem.* **2016**, *808*, 87–96.
- (15) (a) Tauchman, J.; Therrien, B.; Süss-Fink, G.; Štěpnička, P. Heterodinuclear Arene Ruthenium Complexes Containing a Glycine-Derived Phosphinoferrrocene Carboxamide: Synthesis, Molecular Structure, Electrochemistry, and Catalytic Oxidation Activity in Aqueous Media. *Organometallics* **2012**, *31*, 3985–3994. (b) Mannancheril, V.; Therrien, B. Strategies toward the Enhanced Permeability and Retention Effect by Increasing the Molecular Weight of Arene Ruthenium Metallaassemblies. *Inorg. Chem.* **2018**, *57*, 3626–3633. (c) Freudenreich, J.; Dalvit, C.; Süss-Fink, G.; Therrien, B. Encapsulation of Photosensitizers in Hexa- and Octanuclear Organometallic Cages: Synthesis and Characterization of Carceplex and Host–Guest Systems in Solution. *Organometallics* **2013**, *32*, 3018–3033.
- (16) Tafesh, A. M.; Weiguny, J. A Review of the Selective Catalytic Reduction of Aromatic Nitro Compounds into Aromatic Amines, Isocyanates, Carbamates, and Ureas Using CO. *Chem. Rev.* **1996**, *96*, 2035–2052.
- (17) Kim, S.; Choi, H.; Baik, C.; Song, K.; Kang, S. O.; Ko, J. Synthesis of conjugated organic dyes containing alkyl substituted thiophene for solar cell. *Tetrahedron* **2007**, *63*, 11436–11443.
- (18) Kondo, K.; Ogawa, H.; Shinohara, T.; Kurimura, M.; Tanada, Y.; Kan, K.; Yamashita, H.; Nakamura, S.; Hirano, T.; Yamamura, Y.; Mori, T.; Tominaga, M.; Itai, A. Novel Design of Nonpeptide AVP V₂ Receptor Agonists: Structural Requirements for an Agonist Having 1-(4-Aminobenzoyl)-2,3,4,5-tetrahydro-1H-1-benzazepine as a Template. *J. Med. Chem.* **2000**, *43*, 4388–4397.
- (19) (a) Hu, Q.; Chen, J.; Zhang, Z.; Liu, Y.; Zhang, W. Rh-Catalyzed One-Pot Sequential Asymmetric Hydrogenation of α -Dehydroamino Ketones for the Synthesis of Chiral Cyclic trans- β -

Amino Alcohols. *Org. Lett.* **2016**, *18*, 1290–1293. (b) Ruff, A.; Kirby, C.; Chan, B. C.; O'Connor, A. R. Base-Free Transfer Hydrogenation of Ketones Using $\text{Cp}^*\text{Ir}(\text{pyridinesulfonamide})\text{Cl}$ Precatalysts. *Organometallics* **2016**, *35*, 327–335. (c) Tan, X.; Wang, G.; Zhu, Z.; Ren, C.; Zhou, J.; Lv, H.; Zhang, X.; Chung, L. W.; Zhang, L.; Zhang, X. Hydrogenation of Aldehydes Catalyzed by an Available Ruthenium Complex. *Org. Lett.* **2016**, *18*, 1518–1521.

(20) Song, D.-P.; Wang, Y.-X.; Mu, H.-L.; Li, B.-X.; Li, Y.-S. Observations and Mechanistic Insights on Unusual Stability of Neutral Nickel Complexes with a Sterically Crowded Metal Center. *Organometallics* **2011**, *30*, 925–934.

(21) Govender, P.; Renfrew, A. K.; Clavel, C. M.; Dyson, P. J.; Therrien, B.; Smith, G. S. Antiproliferative activity of chelating N,O- and N,N-ruthenium(II) arene functionalised poly(propyleneimine) dendrimer scaffolds. *Dalton Trans.* **2011**, *40*, 1158–1167.

(22) Fan, X.-N.; Deng, W.; Liu, Z.-J.; Yao, Z.-J. Half-Sandwich Iridium Complexes for One-Pot Synthesis of Amides: Preparation, Structure and Diverse Catalytic Activity. *Inorg. Chem.* **2020**, *59*, 16582–16590.

(23) Zhang, J.; Balaraman, E.; Leitens, G.; Milstein, D. Electron-Rich PNP- and PNN-Type Ruthenium(II) Hydrido Borohydride Pincer Complexes. Synthesis, Structure, and Catalytic Dehydrogenation of Alcohols and Hydrogenation of Esters. *Organometallics* **2011**, *30*, 5716–5724.

(24) Halpern, J.; Harrod, J. F.; James, B. R. Homogeneous Catalysis of the Hydrogenation of Olefinic Compounds by Ruthenium(II) Chloride. *J. Am. Chem. Soc.* **1966**, *88*, 5150–5155.

(25) Samec, J. S. M.; Backvall, J. E. Ruthenium-Catalyzed Transfer Hydrogenation of Imines by Propan-2-ol in Benzene. *Chem. - Eur. J.* **2002**, *8*, 2955–2961.

(26) Casey, C. P.; Singer, S. W.; Powell, D. R.; Hayashi, R. K.; Kavana, M. Hydrogen Transfer to Carbonyls and Imines from a Hydroxycyclopentadienyl Ruthenium Hydride: Evidence for Concerted Hydride and Proton Transfer. *J. Am. Chem. Soc.* **2001**, *123*, 1090–1100.

(27) (a) Rai, R. K.; Mahata, A.; Mukhopadhyay, S.; Gupta, S.; Li, P.-Z.; Nguyen, K. T.; Zhao, Y.; Pathak, B.; Singh, S. K. Room-Temperature Chemoselective Reduction of Nitro Groups Using Non-noble Metal Nanocatalysts in Water. *Inorg. Chem.* **2014**, *53*, 2904–2909. (b) Liu, J.; Cui, J.; Vilela, F.; He, J.; Zeller, M.; Hunter, A. D.; Xu, Z. In situ production of silver nanoparticles on an aldehyde-equipped conjugated porous polymer and subsequent heterogeneous reduction of aromatic nitro groups at room temperature. *Chem. Commun.* **2015**, *51*, 12197–12200. (c) Jia, W.-G.; Dai, Y.-C.; Zhang, H.-N.; Lu, X.; Sheng, E.-H. Synthesis and characterization of gold complexes with pyridine-based SNS ligands and as homogeneous catalysts for reduction of 4-nitrophenol. *RSC Adv.* **2015**, *5*, 29491–29496. (d) Zhao, Z.; Yang, H.; Li, Y.; Guo, X. Cobalt-modified molybdenum carbide as an efficient catalyst for chemoselective reduction of aromatic nitro compounds. *Green Chem.* **2014**, *16*, 1274–1281. (e) Yang, X.-J.; Chen, B.; Zheng, L.-Q.; Wu, L.-Z.; Tung, C.-H. Highly efficient and selective photocatalytic hydrogenation of functionalized nitrobenzenes. *Green Chem.* **2014**, *16*, 1082–1086. (f) Sanjini, N. S.; Velmathi, S. Iron impregnated SBA-15, a mild and efficient catalyst for the catalytic hydride transfer reduction of aromatic nitro compounds. *RSC Adv.* **2014**, *4*, 15381–15388. (g) Wienhofer, G.; Sorribes, I.; Boddien, A.; Westerhaus, F.; Junge, K.; Junge, H.; Llusar, R.; Beller, M. General and Selective Iron-Catalyzed Transfer Hydrogenation of Nitroarenes without Base. *J. Am. Chem. Soc.* **2011**, *133*, 12875–12879. (h) Jia, W.-G.; Zhang, T.; Xie, D.; Xu, Q.-T.; Ling, S.; Zhang, Q. Half-sandwich cycloruthenated complexes from aryloxazolines: synthesis, structures, and catalytic activities. *Dalton Trans.* **2016**, *45*, 14230–14237.

(28) Sheldrick, G. M. *SHELXL-97, Program for the Refinement of Crystal Structures*; Universität Göttingen: Germany, 1997.

(29) Sheldrick, G. M. *SADABS (2.01)*, Bruker/Siemens Area Detector Absorption Correction Program; Bruker AXS: Madison, WI, 1998.